

IMECE2007-44088

**MINIATURE PIEZO COMPOSITE BIMORPH ACTUATOR FOR ELEVATED
TEMPERATURE OPERATION**

Charles E. Seeley*

General Electric Global Research Center
Niskayuna, NY, 12309, USA
Email: seeley@research.ge.com

Eladio Delgado

General Electric Global Research Center
Niskayuna, NY, 12309, USA
Email: delgado@research.ge.com

Jan Kunzman

Smart Materials Corp
Dresden, Germany
Email: j.kunzmann@smart-material.com

Dirk Bellamy

GE Industrial - Security
Salem, OR, 97302
Email: dirk.bellamy@ge.com

ABSTRACT

Development of a new, miniature actuator with large stroke and enhanced thermal stability could provide an improved capability for useful applications. This paper investigates the design, fabrication and testing of a macro fiber composite (MFC) based bimorph actuator to meet stringent requirements such as size, stroke and thermal stability. Results indicate that a d_{33}/d_{31} MFC configuration was compact and provided sufficient stroke while avoiding issues related to depolarization at elevated temperature. A compact, high voltage power supply that runs off of a 3 volt battery was also developed as part of this effort

INTRODUCTION

There is a need for small (25×5 mm) actuators that can generate large stroke (1 mm) relative to their size that are stable over a large temperature range (-30 to 70° C) with a small variation (< 0.1 mm) in actuator position over that temperature range and engage within 10 ms. The use of a low power autonomous voltage signal to energize the actuator, such as from a 3 volt camera battery, is desirable to facilitate the interface of the actuator with other systems. Traditional actuators, such as solenoids and pneumatic/hydraulic actuators, do not meet size, power and form

factor requirements while Micro Electronic Mechanical Systems (MEMS) actuation technology does not scale up well in a cost effective manner to the dimensional space available.

The use of shape changing materials for actuators has received considerable attention lately [1]. These materials include shape memory alloys [2, 3], piezoelectric materials [4], electrostatic materials and magnetostrictive [5] materials. Various structural configurations of these materials have been used to amplify the force or stroke to compensate for the limitations of these materials for particular applications. Stroke amplification schemes include placement considerations, tendons and wires, lever arms, inchworms, curved shapes and unimorph/bimorphs. Piezoelectric materials are attractive shape changing materials for some applications because they respond to an electrical input, engage quickly, are capable of a wide frequency range from DC to MHz, produce high force and are readily available. However, they produce only limited stroke and their use at elevated temperature is not well established. Geometric stroke amplification using a bimorph configuration substantially boasts the free deflection of piezoelectric actuators. Further enhancements are obtained using new piezoelectric composite actuators with interdigitated electrodes [6] using a high quality fabrication process [7] known as Macro Fiber Composites (MFCs). MFCs utilize piezoelectric fibers embedded in a dielectric matrix and packaged between

*Address all correspondence to this author.

sheets of metalized polyimide film for the interdigitated electrodes. MFCs have higher output and are more rugged compared to monolithic piezoceramic wafers since the fibers provide directional actuation along their length exploiting the major d_{33} piezoelectric coefficient and the polymer matrix material provides flexibility. A number of previous MFC applications in the fields of shape control [8], vibration and noise cancellation [9] as well as online health monitoring [10] and energy harvesting [11, 12] show the outstanding potential of this actuator type.

This paper will discuss the design, fabrication and characterization of a miniature bimorph MFC actuator to meet demanding geometric, temperature and response time requirements. The bimorph actuator is designed to fit in a small space. Materials and dimensions are optimized using a finite element model. The MFCs are laminated to a substrate during fabrication. A power supply that runs off of a 3 volt battery was developed for the bimorph actuator. Characterization tests at room temperature and elevated temperature indicate performance that meets the difficult size, stroke and thermal requirements.

DESIGN AND MODELING

The bimorph actuator developed for this investigation is shown in Fig. 1. It comprised a substrate material with MFCs bonded to both sides and energized out of phase to produce out of plane deflection. A finite element analysis (FEA) model of the bimorph actuator was created using MSC/NASTRAN to study the parameters that determine the bimorph actuator's performance such as the influence of material and geometric parameters.

Although the bimorph actuator is simple in concept, it has several subtle features that impact the performance. For example, the adhesive used to bond the MFCs to the substrate has finite thickness and elastic properties that influence the transfer of induced strain from the piezoelectric fibers to the substrate. The side bar bus that connects the interdigitated electrode pattern results in a non active region along the side of the bimorph that increases the bending stiffness without adding any actuation authority, thus reducing the overall stroke. This issue tends to be more of a factor in smaller devices, such as the one developed in this effort. The FEA model enabled the actual planar geometry of the bimorph to be analyzed, including differences between the active area and the substrate area. The model utilized multilayer composite shell elements to incorporate effects of the piezoelectric and substrate layers and the orthotropic material properties of the MFCs. Clamped boundary conditions were applied on one end, and deflection due to energizing the MFCs was measured at the opposite end. The induced piezoelectric strain was simulated with an analogous thermal strain in the model. Ten elements were used across the width of the actuator and 35 elements were used along the length. The static solution took less

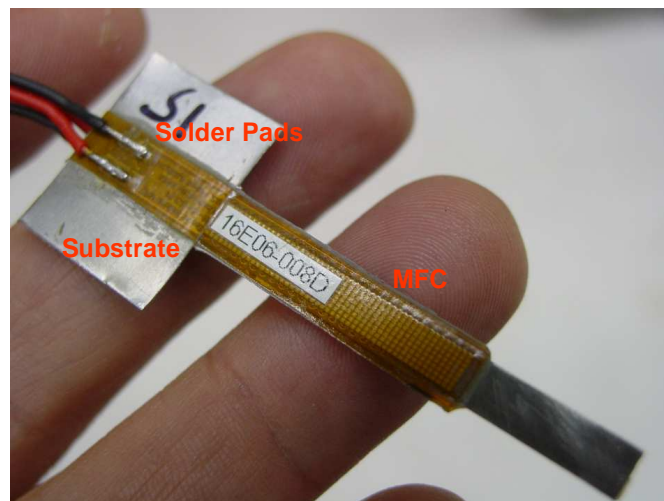


Figure 1. Completed miniature bimorph actuator showing customized MFCs and substrate material. Extra substrate material will be trimmed off for actual product integration

than one minute of CPU time on a modern personal computer (PC).

FEA model results are presented in Table 1. Here, free displacements (stroke) and block forces at full power are shown for a variety of configurations, substrate materials and thicknesses. In addition to the bimorph configuration (B), where the top and bottom active layers were energized out of phase to create a bending moment, monomorph configurations (M), with only a single active layer bonded to a substrate, were also included for comparison. It was observed from these results that a monomorph generated substantial stroke due to the reduced bending stiffness from the absence of a second active layer. However, it was problematic from the point of view of thermal stability since it was not symmetric and the coefficients of thermal expansion for both the substrate and active material must be matched exactly to avoid unwanted stroke from an environmental temperature change. Therefore, the monomorph configuration was included here only for comparison. It was interesting that the monomorph produced greater deflection for the same substrate material, even though only one MFC was present. This was due to the reduced bending stiffness with just one MFC present. In general, it was observed that the total stroke was a strong function of the bending stiffness that was in turn a function of both the substrate modulus and substrate thickness. A thinner substrate was found to improve stroke, although with a corresponding trade-off in the block force. A more compliant substrate material also tended to improve the stroke, although too compliant a material may not be optimal due to excessive shear deformation in the limiting case. Based on this analysis, the steel substrate was selected as the primary substrate material due to its combination of reason-

able stroke characteristics from the table below, high blocking force, the ease with which it could be machined into the desired dimensions, common availability and low cost.

FABRICATION

This section describes the actuator fabrication and the implementation of the power supply.

Actuator Fabrication

Actuator fabrication, whether monomorph or bimorph, occurred in two primary steps. The first step was to create the piezoelectric devices using the MFC fabrication process [7], and the second step was to bond them to the substrate material. A top view of the drawing for the MFCs is shown in Fig. 2. The MFC was customized using a standard Smart Materials Corp MFC as a basis for the new bimorph actuator and included several important design features. First, the active area was made to fit within the specified geometric envelope. The interdigitated electrodes all had rounded corners to minimize electrical field concentrations and the potential dielectric breakdown. An inactive area was included to facilitate clamping for easy evaluation and handling. Solder pads were incorporated for electrical power connections. Initially, piezoelectric fibers were created by dicing a monolithic wafer of piezoceramic material with dicing tape as a backing to maintain fiber alignment. In parallel, the electrode pattern was deposited on the Kapton film according to the drawing in Fig. 2. Next, one side of the piezoelectric fibers was bonded to one Kapton sheet by partially curing the dielectric adhesive. The dicing tape was removed at this point since the B-staged adhesive now held the alignment, and the second Kapton sheet was bonded to the other side of the piezoelectric fibers with the cure cycle run to completion for both sides. A vacuum press was used to create the elevated temperature and pressure required to cure the adhesive and eliminate air entrapment in the laminate. Polarization of the MFCs to induce their piezoelectric properties by subjecting them to a high electric field generated at 1500 Volts for several minutes completed the first step. The MFCs were bonded to the substrate material in the second step. A vacuum bag was used to cure the MFC-substrate adhesive. Here, rigid caul plates were used to provide uniform pressure to the laminate during cure with press pads that provide compliance to avoid stress concentrations on uneven surfaces that could damage the part. The cross section of Fig. 3 shows the piezoelectric layers relative to the substrate. The relative thickness of the bond lines was also observed and found to have a significant impact on performance. The alignment of the top and bottom interdigitated electrodes within an MFC was found to be satisfactory. The waviness of the Kapton layers was due to extra adhesive that was squeezed out during cure and was beneficial due to the reduced bond line thickness that improved induced strain transfer to the

substrate in these regions. A completed actuator is shown in Fig. 1. The extra substrate material at the clamped end helped with handling the miniature device and did not effect the performance in any way. It would be trimmed off for actual product integration.

PZT 5A is a widely used piezoceramic material due to its common availability and a good balance between its mechanical and piezoelectric properties. It is the most common material used in MFC fibers. PZT 5H is also a commonly available piezoceramic material and has higher piezoelectric coupling, although its mechanical properties are not as good as PZT 5A. There was interest in evaluating PZT 5H for use in the bimorph actuator because the higher piezoelectric coupling could possibly improve the stroke. Several attempts were made to fabricate MFCs with PZT 5H instead of PZT 5A in an attempt to obtain these benefits. Unfortunately, cracks occurred in some of the PZT 5H samples from the lamination process that results in mechanical and/or dielectric failure. This indicated the need for further process development with the 5H material to improve yields.

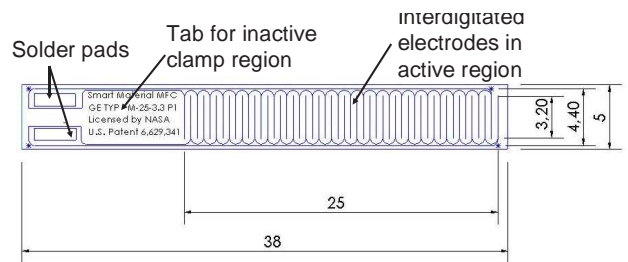


Figure 2. Top view drawing of MFC showing the active area of interdigitated electrodes. Electrode corners are rounded to reduce electric stresses

POWER SUPPLY

A low power, high voltage power supply circuit was designed to support the prototype development of the miniature bimorph actuator. The design requirements for the prototype actuator power supply included obtaining power from a small CR2 3 volt camera battery that would provide a minimum of 1000 actuations at 1500 VDC for an average of 5 seconds per actuation. The requirement also included consideration of electronics small enough to meet stringent space requirements. Furthermore, the power supply output response had to be fast enough to provide full actuation stroke within 10 ms, and it had to be low cost and simple with minimal parts count.

Table 1. Finite Element Model results for various monomorph (M) and bimorph (B) configurations

Configur- ation	Substrate Material	Substrate Thickness, <i>mm</i>	V_{top} , V	V_{bot} , V	Free Displacement, <i>mm</i>	Block Force, <i>mN</i>
M	steel	0.1	1500	-	1.54	0.35
M	steel	0.2	1500	-	1.09	0.50
B	none	-	1500	0	1.09	0.40
B	none	-	1500	-500	1.44	0.53
B	steel	0.1	1500	-500	1.16	0.69
B	steel	0.2	1500	-500	0.90	0.82
B	polymer	0.1	1500	-500	1.20	0.68
B	polymer	0.2	1500	-500	1.01	0.86

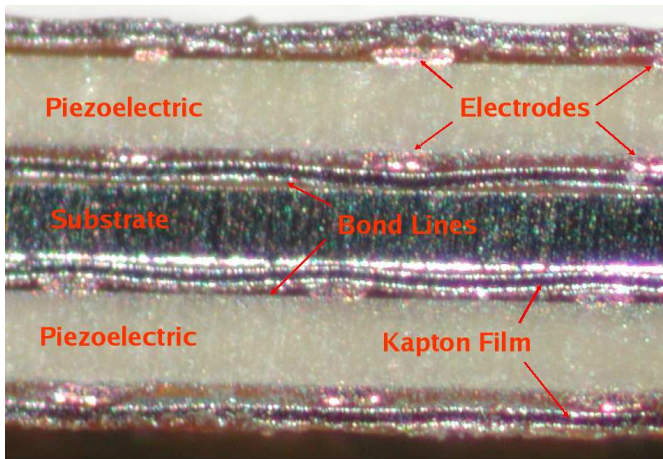


Figure 3. Cross section of bimorph actuator showing piezoelectric and substrate layers. The interdigitated electrodes were found to have good alignment from top to bottom and the bond line thicknesses were found to be significant relative to the MFC and substrate thicknesses

Circuit Design

A flyback topology was selected to implement the low power high voltage supply. This approach was similar to the power electronics that are used to drive cathode ray tube (CRT) television sets and automobile ignition systems. Unlike a normal transformer that directly couples energy from one winding to another winding, a flyback transformer first stores energy received from the input power supply (charging portion of a cycle) and then transfers energy (discharge portion of a cycle) to the output, that is usually a diode and a storage capacitor with a load connected across its terminals. Figure 4 shows the block diagram of the approach selected. For this topology, a wide range of low cost single integrated circuits (ICs) solutions were readily available that could be used to implement the controller. An MIC3172

switching regulator controller IC was selected for its operating frequency of 100KHz and for its output switch ratings of 65 V and 1.65A. This controller also had the ability to be turned on and off to conserve energy. Components become bulky, expensive and hard to obtain when voltage ratings exceeded 1000 V. To mitigate this problem, a series connected high voltage tandem flyback (HVTF) output design was developed. This tandem output approach consisted of two flyback transformers whose input winding were connect in parallel and with outputs connected in series. This approach forced the power supply voltage to be centered about an electrical common, thus reducing the voltage stress on the output components. The output voltage developed with the HVTF circuit was 900 V from common to positive lead and 715 V from common to negative terminal as measured from the prototype developed. Another advantage of the HVTF approach was the ability to interconnect multiple actuators. The output voltage configuration allowed for an actuator to be connected from negative to positive terminals having up to 1615 V available. Another possible connection was to have two actuators connected such that one was attached from the common to positive with 900 V and the other connected from common to the negative terminal with a voltage of 715 V. Thus, this topology allowed for various actuator interconnections and voltage levels from a single high voltage power supply.

A PSPICE [13] circuit simulation was used to verify the design of the HVTF power supply. The design was optimized for voltage output, signal response, and power consumption. Various simulations were conducted to select the proper flyback transformer turns ratio and to optimize output response to meet the desired specifications. PSPICE results showed that the power supply output charged to full voltage within 2.0 ms. This was later confirmed. The output voltage level reached the ideal maximum of 2000 V measured from the negative to positive terminal.

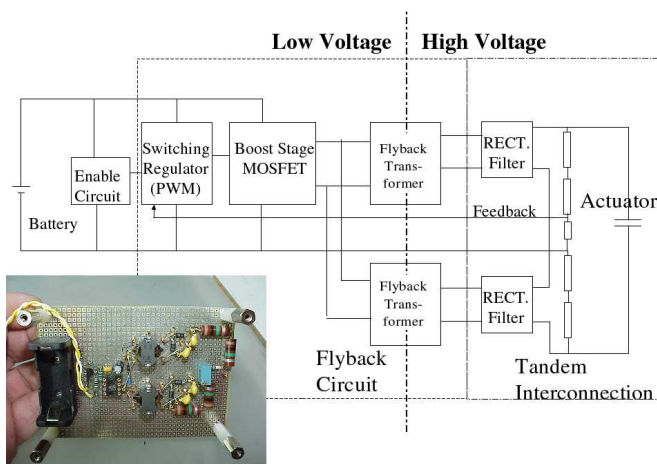


Figure 4. Block diagram of the high voltage tandem flyback (HVTF) circuit power supply with low power consumption and the prototype circuit

Results

The HVTF circuit design was implemented using component values and transformer parameters obtained from the simulations. A controller, along with the associated enable circuit and higher current driver were included. Output filter/holding capacitors were later added to the original circuit to improve stability. Voltage feedback was obtained from a voltage divider on the positive output section, and the voltage divider potentiometer allowed for reasonable adjustment of the output voltage. Operation of the HVTF power supply was controlled by a toggle switch. In the open position, the controller was forced into sleep mode to conserve energy. An output driver stage monitors was installed during the debugging phase to preview the controller output stage and check for an over current limit during the start-up operating sequence. The HVTF power supply was built with commercial-off-the-shelf (COTS) components readily available and low in cost, although the transformers required some customization. The pair of transformers in the prototype were designed using Ferroxcube RM5/I-3f3 cores having 5 turns on the primary and 200 turns on the secondary. A single transformer design with multiple output windings could reduce transformer size and parts count for high volume manufacturing. Leaded components were used to build the prototype since these were readily available and size was of secondary importance for the initial prototype. Further miniaturization could be achieved using surface mount components on a printed circuit board assembly (PCA). Despite the larger leaded components, the final size of the initial HVTF prototype, shown in Fig. 4, was surprisingly small considering the large voltage (1650 V) generated. The prototype HVTF circuit was placed inside an insulated project box for safety.

Figure 5 shows an oscilloscope trace of the working prototype waveforms at the end of the startup sequence. The scope trace shows the output voltage at 1200 V, the driver stage drain switching at 100kHz, the ramping of the primary current and the output current of the positive section. All the operating requirements were achieved with the design. The developed bimorph actuator was connected to the HVFT power supply output and energized. Deflection measurements indicated that the actuator met the deflection requirements as shown in Fig. 6.

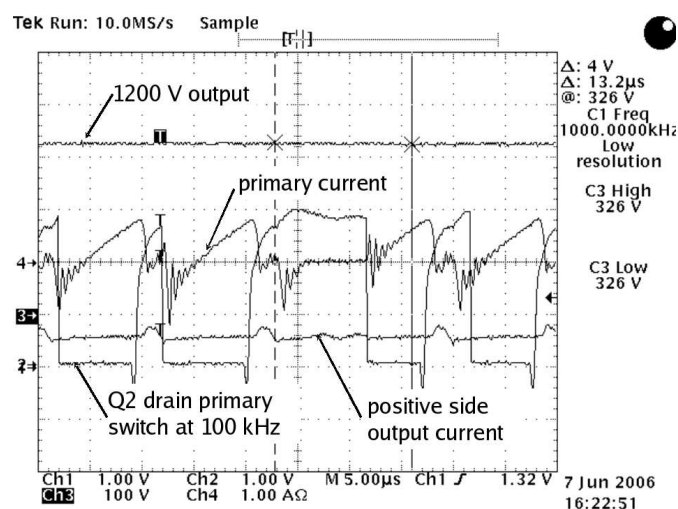


Figure 5. Oscilloscope output of the HVTF power supply prototype

RESULTS

This section discusses the results and lessons learned from the fabrication and characterization of the new, MFC based miniature actuators. The test setup for determining actuator performance is described first. Following the test setup is a discussion of actuator characteristics at room temperature and elevated temperature.

Actuator Characterization

An experimental apparatus was designed and constructed to characterize the miniature bimorph actuators as shown in Fig. 7. Measurements were taken to obtain the stroke of the actuator as a function of voltage and temperature. Recall that the requirements are an actuation stroke of $> 1.0 \text{ mm}$ with $< 0.1 \text{ mm}$ of deflection due to changes in temperature. The apparatus comprised a clamp to hold the Device Under Test (DUT), film heaters powered by a DC power supply to raise the ambient temperature, an environmental chamber to stabilize the temperature, a thermocouple

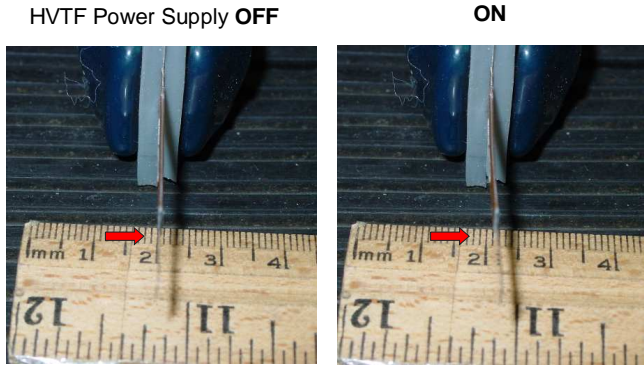


Figure 6. Bimorph MFC actuator with HVTF power supply OFF, and greater than 1 mm deflection with it ON

to measure the air temperature next to the actuator and a laser displacement measurement system. A hole was made in the environmental chamber for the laser to pass through. Initially, three orthogonally placed film heaters were used. However, it was determined that the asymmetry in the heat flux from the heaters created an undesirable temperature gradient across the DUT, so the heater configuration was reduced to two symmetrically placed heaters.

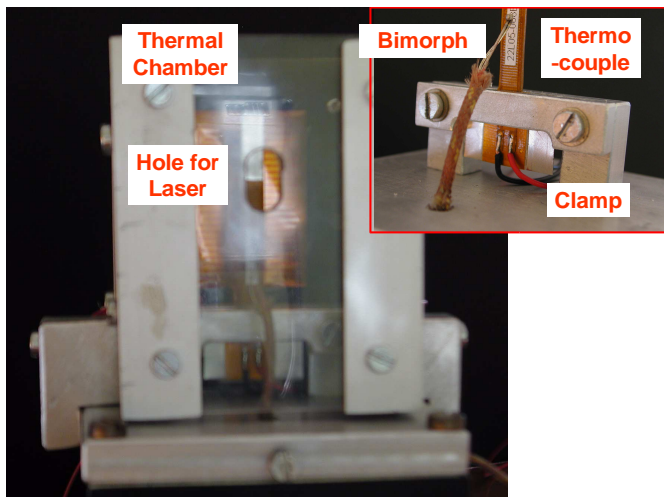


Figure 7. Experimental apparatus used to characterize various designs of the miniature actuators

Room Temperature Results

A total of 10 actuators were fabricated to investigate the effects that various parameters had on the maximum stroke as shown in Table 2. The parameters investigated were the piezoelectric material (A,H), the MFC configuration (P1/P1,P1/P2), the substrate material (M1,M2), the total thickness, the MFC adhesive (LTM,HTM), the substrate adhesive (LTS,HTS), and the operating voltage. The stroke was determined by cycling between zero volts and a specified voltage, then recording the average difference in position from minimum to maximum voltage over several cycles.

Bimorph actuators with MFCs fabricated using PZT 5A (A) fibers were compared to PZT 5H (H). The H material was expected to give higher stroke due to higher piezoelectric properties, but there was a risk of potential issues due to lower mechanical properties and fabrication issues. Two MFC configurations were investigated, P1/P1 and P1/P2 as shown in Fig. 8. In the P1/P1 configuration, the top MFC is driven with a positive electric field (E) along the direction of the piezoelectric polarization (P) creating a positive strain (S) and exploiting the major d_{33} piezoelectric coefficient. The lower MFC is also a P1, but is driven with a negative electric field against the direction of piezoelectric polarization to induce a negative strain and a net bending moment to induce out of plane deflection. In the P1/P2 configuration, the top MFC is also driven as before with a positive electric field along the direction of polarization to create a positive strain. However, the bottom MFC is a P2 type that is driven with a positive out of plane electric field along the direction of out of plane polarization to create a negative in plane strain and net bending moment exploiting the minor d_{31} coefficient instead. Therefore, the P1/P1 configuration creates a bending moment from opposite voltages while the P1/P2 configuration creates a bending moment from the orientation of the piezoelectric polarization. A P1/P1 configuration with no substrate was also included for comparison, since it was the limiting case of zero substrate stiffness. Two substrate materials, that were varieties of the low thermal expansion alloy Kovar, (M1,M2), were included in the investigation. The standard adhesive for off-the-shelf MFCs was Loctite E120HP epoxy. It was considered a low temperature (LTM) adhesive since it tended to soften above 50° C. Another MFC adhesive, Huntsman HT (HTM), was evaluated due to its potentially superior mechanical properties at elevated temperature. Two adhesives used to bond the MFCs to the substrate were also examined. The Loctite E120HP (LTS) and a high glass transition temperature epoxy with filler, Loctite E214HP, that was expected to have superior high temperature properties, was used here. Several operating voltages were investigated using 1500/0 V as a baseline. Here, the notation indicates that 1500 V, a typical maximum MFC voltage, was applied to the top MFC while 0 V was applied to the bottom MFC. The effect of energizing the bottom MFC was included as a 1500/-500 V case for the P1/P1 configuration and 1500/260 V for the P1/P2 case. The effect of

higher than typical voltage applied to the top MFC was included as the 1850/0 V case. Although it gave greater stroke, the higher voltage risked dielectric breakdown. Note that the applied voltage is indicated here, rather than the electric field (V/m). This is because the voltage was specified directly while the electric field was not known exactly due to variations in the field between the interdigitated electrodes.

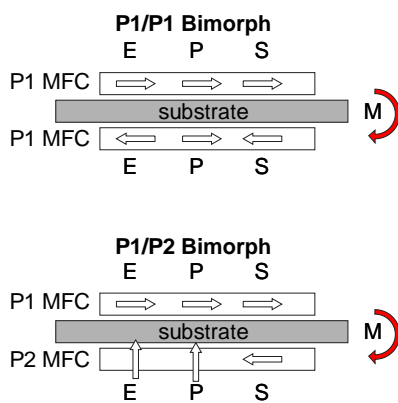


Figure 8. P1/P1 and P1/P2 bimorph configurations. P1/P1 configurations utilizes opposite voltage to create bending moment while P1/P2 exploits directional piezoelectric properties to create bending moment so that electric field is always aligned with polarization to avoid depoling

Many interesting design trends were found from the test results. These results were also averaged over particular sets of parameters as shown in Table 3 to identify trends. For example, the average stroke of the H material was found to be about the same as the A material. However, the H material devices were more problematic to fabricate and were not as rugged, so the A material was considered optimal. The stroke using the M2 substrate was consistently better than the M1 material, so the M2 material was considered best. Although the stroke from the bimorph with no substrate was very good, it was not clear how the actuator would be mounted or integrated into the final system without it, so this option was not considered practical. The best stroke was obtained from the P1/P2 configuration, although the geometry of the MFCs used for this sample was based on stock MFC sizes of 28 by 14 mm and may not include size effects of the smaller 25 by 10 mm MFCs used for the rest of the bimorphs evaluated. The high temperature MFC adhesive HTM gave lower stroke compared to the low temperature LTM, but provided thermal stability and may be a good option if selection of the other design parameters enables a stroke of greater than the target of

1 mm. It was learned that the shear strength and thermal stability of the adhesive layers was important for the thermal stability of the entire bimorph. Therefore it was recommended to use the HTS adhesive to bond the MFCs to the substrate. Although only a limited number of actuators with HTS adhesive were considered, it was observed that these devices were somewhat thicker than the devices that used the LTS adhesive, possibly due to the greater uncured viscosity and filler in the HTS material. There was a general trend towards reduced stroke at increased thickness due to the increased bending stiffness regardless of the adhesive. This indicated that fabrication process parameters must be carefully monitored to ensure the thinnest possible bond line. A driving voltage of 1500 V was known to be reliable while there was a risk of dielectric breakdown above 2000 V. These problems could be exacerbated from electric stress concentrations due to the small size of the actuator, although operative voltages as high as 4000 V have been reported as successful. However, the reliability at these high voltages is unknown. All of the bimorph actuators were energized with a nominal voltage of 1500/0 V for comparison. The stroke at room temperature was improved by simultaneously energizing the bottom MFC to -500 V (1500/-500 V). For example, the "A,P1/P1,M2,LTM-LTS" sample showed a 20% gain in stroke when the bottom MFC was energized compared to the nominal case. Increasing the top MFC voltage to 1850 V (1850/0 V) also improved the stroke by 9%. The combination of increased top MFC voltage and energizing the bottom MFC to 1850/-500 V is estimated to yield a stroke of 1.17 mm for this particular bimorph actuator. This represents an improvement of 20% compared to the nominal case. The P1/P2 configuration was considered best since it minimized the risk of depolarization at elevated temperature by driving both top and bottom MFCs at maximum voltage, to maximize the induced strain, in the direction of their respective polarization, but exploiting the sign of the d_{31} versus d_{33} coefficients to create the bimorph bending moment. It was also observed that the first cycle differed substantially from the rest of the cycles that tended to converge over stable hysteresis loop. Therefore, a "burn-in" procedure may be required for new actuators prior to installation. Due to resource restrictions, it was not possible to evaluate replicates of each design, so variability in performance within a single design is unknown.

Elevated Temperature Results

The bimorph actuators were evaluated at elevated temperature to determine the effect temperature had on the actuator stroke, and also the effect that the change in temperature had on producing unwanted actuation due to thermal expansion. Elevated temperature potentially impacted the stroke in several ways. It could cause the polarized state of the piezoelectric material to become unstable resulting in reduced piezoelectric properties and actuation authority over time. The resistance of the

Table 2. Actuator stroke results for various designs at room temperature

Piezo Mat'l	Config.	Substrate Mat'l	Thick., <i>mm</i>	Adhesive	Stroke, <i>mm</i>		
					1500/0 <i>V</i>	1500/-500 <i>V</i>	1850/0 <i>V</i>
A	P1/P1	M1	0.83	LTM-LTS	0.74	0.93	0.84
A	P1/P1	M2	0.72	LTM-LTS	0.91	1.09	0.99
A	P1/P1	M1	0.83	HTM-LTS	0.44		0.50
A	P1/P1	M2	0.82	HTM-LTS	- ^a	-	-
H	P1/P1	M1	0.83	LTM-LTS	0.66	0.79	0.75
H	P1/P1	M2	0.80	LTM-LTS	0.93	0.99	1.02
H	P1/P1	M1	0.93	HTM-HTS	0.57		0.64
H	P1/P1	M2	0.91	HTM-HTS	0.64		0.74
A	P1/P1	none	0.68	LTM-LTS	1.19		1.34
A	P1/P2	M1	0.77	LTM-HTS	0.98		1.41 ^b

^adielectric breakdown^b1500/260 *V*Table 3. Actuator average stroke results at room temperature and 1500/0 *V*

Actuator Parameter	Stroke, <i>mm</i>
Piezo Material: A,H	0.74,0.73
Configuration: P1/P1, P1/P2	0.77,1.41
Substrate Material: M2,M1	0.85,0.63
Adhesive: LTM,HTM	0.80,0.55

piezoelectric material could drop at higher temperatures resulting in higher current draw and possible self heating. The mechanical property for the adhesive for both the MFC and bonding of MFCs to the substrate could be degraded. This could interfere with the transfer of strain from the piezoelectric fibers to the substrate resulting in degraded actuator performance. Creep could occur over time that resulted in a residual stress that the piezoelectric material must overcome, again reducing the actuation authority. The dielectric properties of the MFCs could degrade at elevated temperature risking catastrophic dielectric breakdown. All of the bimorph actuators were designed to be symmetric about the neutral axis so that thermal expansion of the component materials would be balanced and cancel out stresses that could induce out of the plane bending to meet the 0.1 *mm* thermal deflection requirement. In practice, the bimorph actuators were not per-

fectly symmetric due to manufacturing variability. This led to unwanted out of plane bending from thermal expansion due to temperature change and created an undesirable, uncontrollable actuation that could be problematic if it exceeded the requirement.

Results for the elevated temperature tests are presented in Table 4 and Figs. 9 and 10. The bimorph actuators were selected from the same group used in the room temperature tests discussed previously. Effects of various actuator parameters, such as the piezoelectric material (A,H), MFC configuration (P1/P1,P1/P2), substrate material (M1,M2) and operating voltage (1500/0, 1500/-500, 1500/260 *V*) were considered. The same MFC adhesive (LTM) and substrate adhesive (LTS) was used in all elevated temperature cases. The stroke was determined at various temperatures between room temperature and 75°C. Three temperatures (25, 50, 75°C) were selected for comparison in Table 4. The test was conducted by heating up the bimorph actuators to the specified temperature using the test apparatus described earlier, waiting several minutes for the actuators to reach thermal steady-state, then energizing the MFCs. Initially both top and bottom MFCs were de-energized (0/0 *V*). Next, the top MFC was energized to 1500 *V* while the bottom MFC remained de-energized (1500/0 *V*). Then, the bottom MFC was energized to -500 *V* (1500/-500 *V*) for the P1/P1 configuration and 260 *V* (1500/260 *V*) for the P1/P2 configuration. The stroke was calculated as the difference in measured position between voltage states as before. The measured stroke, U_{meas} , was assumed to be

a function of three quantities as follows

$$U_{meas} = U_{clamp} + U_{therm} + U_{piezo} \quad (1)$$

where U_{clamp} was the thermal distortion due to the clamp, U_{therm} was the distortion due to thermal expansion mismatch of the actuator itself, and U_{piezo} was the stroke due to piezoelectric actuation. The distortion due to the clamp was determined to be roughly $0.002 \text{ mm}/^{\circ}\text{C}$ from preliminary tests. The thermal distortion, U_{therm} , was found to be on the order of 10% of U_{piezo} . Therefore, the stroke results presented in Table 4 were the measured values, U_{meas} , for simplicity since the stroke due to piezoelectric actuation, U_{piezo} was of primary interest here and it dominated the value of U_{meas} .

Results indicated that the temperature had a noticeable impact on the stroke. Surprisingly, the stroke increased substantially with temperature at the 1500/0 V operating voltage. The stroke increased approximately 8% for the A piezoelectric material and nearly 40% for the H material over the temperatures studied indicating that the H material was more sensitive to the elevated temperature. The sensitivity of the H material made the design of a robust stable bimorph actuator more difficult. So again, the A material had better qualities for the piezoelectric fiber material selection. Although the mechanical properties of the critical adhesives may have degraded somewhat at higher temperature, they were still able to transfer sufficient strain from the piezoelectric fibers to the substrate to induce bending. The reduction in stiffness from the adhesive enabled greater deflection from the same induced strain produced by the MFCs. The LTM-LTS combination was most likely more flexible than the HTM-HTS adhesives at room temperature giving the actuator more compliance and higher stroke. The LTM-LTS combination was selected as the best set of adhesives. The M2 substrate material yielded 20% better stroke for the A piezoelectric material samples at 75°C compared to the M1 material, confirming the selection of M2 as the substrate material also found optimal in the room temperature tests.

Energizing the bottom MFC in the P1/P1 configuration had unexpected consequences as shown in Fig. 9. Although depolarization of P1 MFCs did not occur until below -500 V at room temperature, the magnitude of the depolarization voltage was reduced since substantially at elevated temperature, and also surprisingly low elevated temperature at that. Significant reduction in stroke was observed in some cases as low as 40°C due to depolarization of the bottom MFC. At 70°C , depolarization was complete and energizing the bottom MFC had no benefit beyond the 1500/0 V voltage case. To make matters worse, the bottom MFC experienced a repolarization in the opposite direction above 70°C and started to work against the top MFC. At 80°C , the bimorph actuator acted as though the bottom MFC was energized with the wrong voltage since the stroke was significantly less than that

with the bottom MFC de-energized. All of the P1/P1 configurations experienced this depolarization/repolarization upon actuation of the bottom MFC at elevated temperature and suffered average reduction in stroke of 17% at 75°C . This surprising result indicated that it was better not to energize the bottom MFC in the P1/P1 configuration if elevated temperature is present and use a 1500/0 V operating voltage instead.

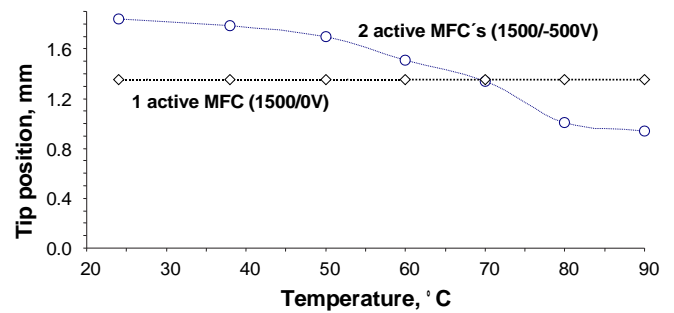


Figure 9. P1/P1 Bimorph actuator stroke vs. temperature. The bottom MFC experiences depolarization and subsequent domain reversal at elevated temperature resulting in lower overall stroke than if only the top MFC was energized

The P1/P2 configuration did not exhibit the same problems experienced by the P1/P1 configuration at elevated temperature. This was because the bottom MFC was energized with a positive voltage along the direction of polarization, for both the top and bottom layers, so that there was no possibility of depolarization or domain reversal. In fact, energizing the bottom MFC for the P1/P2 configuration gave an increase in stroke of 35% at 75°C compared to an average 17% decrease for the P1/P1 configuration at this same temperature. Clearly, the P1/P2 configuration was a better choice in terms of stroke and elevated temperature.

In addition to stroke, thermal stability was investigated to determine the amount of unwanted actuation from thermal expansion due to temperature change. Using Eqn. 1, the thermal deflection, U_{therm} , was calculated using values of U_{meas} , U_{clamp} and U_{piezo} from previous tests. A summary of the results is plotted in Fig. 10 along with the spec limit $\pm 0.1 \text{ mm}$. It was observed that there was noticeable thermal deflection for all of the bimorph actuators due to thermal expansion and the variation in stroke due to the thermal deflection increased with temperature. In some cases the thermal deflection exceeded the spec limit of

Table 4. Actuator stroke results for various designs at elevated temperature

Piezo Mat'l	Config.	Substrate Mat'l	Adhesive	Temp. °C	Stroke, mm	
					1500/0 V	1500/-500 V
A	P1/P1	M1	LTM-LTS	25	0.74	0.93
				50	0.81	0.92
				75	0.81	0.74
A	P1/P1	M2	LTM-LTS	25	0.91	1.09
				50	0.97	1.02
				75	0.97	0.77
H	P1/P1	M1	LTM-LTS	25	0.66	0.77
				50	0.73	0.77
				75	1.08	0.94
H	P1/P1	M2	LTM-LTS	25	0.93	0.99
				50	1.05	1.01
				75	1.08	0.94
A	P1/P2	M1	LTM-LTS	25	0.98	1.41 ^a
				50	0.98	1.40 ^a
				75	0.98	1.34 ^a

^a1500/260 V

± 0.1 mm. However, there did not appear to be any trends among the piezoelectric material (A,H), MFC adhesive (LTM,HTM), or substrate material (M1,M2). The average value of the thermal deflection among all of the actuators tested here was also plotted in Fig. 10. The average value stayed well within the spec limits suggesting that the characteristics of the bimorph actuators that lead to unwanted thermal deflection, such as slight variations in symmetry about the neutral axis from fabrication tolerances, were random variables. Perhaps improvements and fabrication charges would reduce the actuator stroke variation due to thermal deflection.

1 SUMMARY

Bimorph actuators using MFC's were analyzed, fabricated, tested and evaluated for use in space constrained applications. An overview of available actuation technology and shape changing materials identified macro fiber composite (MFC), actuators as suitable for this application. Results from a finite element model indicated promising performance and helped to guide material and geometric parameters. Actuator fabrication was followed by characterization at room temperature and elevated tem-

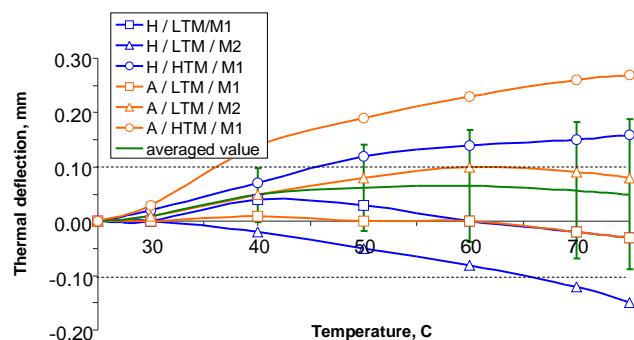


Figure 10. Actuator deflection due to temperature change.

perature. A high voltage power supply that works off of a 3 volt camera batter was also developed and tested. A PZT 5A piezo-

electric material, M2 substrate material, P1/P2 MFC configuration was found to exceed the stroke requirement while mitigating issues related to depolarization at elevated temperature.

ACKNOWLEDGMENT

Special thanks to Scott Smith, Todd Anderson and Chuck Wolfe from GE Global Research and Thomas Daue from Smart Materials Corp.

REFERENCES

- [1] Stevens, T., 1991. "Structures get smart". *Materials Engineering*, Oct., pp. 18–20.
- [2] Lagoudas, D. C., Moorthy, D., Qidwai, M. A., and Reddy, J. N., 1997. "Modeling of the thermomechanical response of active composite laminate with sma layers". *Journal of Intelligent Material Systems and Structures*, **8**, pp. 476–488.
- [3] Scoby, S., and Chen, Y., 2006. "Dynamic behavior of ferromagnetic shape memory alloys". In AIAA/ASME/ASCE/AHS/ASC 47th Structures, Structural Dynamics and Materials Conference. AIAA 2006-1768.
- [4] Niezrecki, C., Brei, D., Balakrishnan, S., and Moskalik, A., 2001. "Piezoelectric actuation: state of the art". *Shock and Vibration Digest*, **33**(4), pp. 269–280.
- [5] Chiang, K. S., Kancheti, R., and Rastogi, V., 2003. "Temperature-compensated fiber bragg grating based magnetostrictive sensor for dc and ac currents". *Opt. Eng.*, **42**(7), pp. 1906–1909.
- [6] Bent, A. A., and Hagood, N. W., 1993. "Development of piezoelectric fiber composites for structural actuation". In AIAA/ASME/ASCE/AHS Structures, Structural Dynamics and Materials Conference, Vol. 34, pp. 3625–3638.
- [7] Wilkie, W. K., Bryant, R. G., High, J. W., Fox, R. L., Hellbaum, R. F., Jalink, A., Little, B. D., and Mirick, P. H., 2000. "Low-cost piezocomposite actuator for structural control applications". In SPIE's 7th Annual International Symposium on Smart Structures and Materials.
- [8] Daue, T., and Kunzman, J., 2006. "New MFC-piezoactuators for optimized systems". In 47th ICAT/JTTAS Joint International Smart Actuator Symposium.
- [9] Sodano, H., Park, G., and Inman, D., 2004. "An investigation into the performance of macro-fiber composites for sensing and structural vibration applications". *Mechanical Systems and Signal Processing*, **18**, pp. 683–697.
- [10] Matt, H., Bartoli, I., di Scalea, F., Park, G., and Farrar, C., 2006. "Health monitoring of uav wing skin-to-spar joints using macro fiber composite transducers".
- [11] Daue, T., and Kunzman, J., 2007. "MFC-piezoactuators

for optimized energy harvesting systems". In Piezoelectric Energy Harvesting Workshop.

- [12] NANOTRON GMBH, 2006. *Nano Net: Product information material*. Germany.
- [13] CADENCE INC., 2005. *PSPICE 9.1 USER MANUAL*.